Veterinary Pathology
49(2) 372-385

DOI: 10.1177/0300985811409443
http://vet.sagepub.com

# Neoplastic and Nonneoplastic Liver Lesions Induced by Dimethylnitrosamine in Japanese Medaka Fish

**K. R. Hobbie[1], A. B. DeAngelo[2], M. H. George[2], and J. M. Law[3]**

## Abstract

Small fish models have been used for decades in carcinogenicity testing. Demonstration of common morphological changes associated with specific mechanisms is a clear avenue by which data can be compared across divergent phyletic levels. Dimethylnitrosamine, used in rats to model human alcoholic cirrhosis and hepatic neoplasia, is also a potent hepatotoxin and carcinogen in fish. We recently reported some striking differences in the mutagenicity of DMN in lambda cII transgenic medaka fish vs. Big Blue® rats, but the preneoplastic and neoplastic commonalities between the two models are largely unknown. Here, we focus on these commonalities, with special emphasis on the TGF-$\beta$ pathway and its corresponding role in DMN-induced hepatic neoplasia. Similar to mammals, hepatocellular necrosis, regeneration, and dysplasia; hepatic stellate cell and "spindle cell" proliferation; hepatocellular and biliary carcinomas; and TGF-$\beta$1 expression by dysplastic hepatocytes all occurred in DMN-exposed medaka. Positive TGF-$\beta$1 staining increased with increasing DMN exposure in bile preductular epithelial cells, intermediate cells, immature hepatocytes and fewer mature hepatocytes. Muscle specific actin identified hepatic stellate cells in DMN-exposed fish. Additional mechanistic comparisons between animal models at different phyletic levels will continue to facilitate the interspecies extrapolations that are so critical to toxicological risk assessments.

## Keywords

Japanese medaka, *Oryzias latipes*, hepatocarcinogenesis, dimethylnitrosamine, aquatic animal models, comparative carcinogenesis, alternative animal models

Exposure to an archetypal carcinogen does not guarantee archetypal histopathology results, especially when comparing animal models as different as fish and rats. Nitrosamines have been one of the most commonly used experimental liver carcinogens, perhaps because of their reliability, potency, and water solubility. Dimethylnitrosamine (DMN) is an alkylating agent well known as both a carcinogen and an inducer of an alcoholic cirrhosis–like condition in the rat. However, although many fish studies have used diethylnitrosamine (DEN), only a few studies have been reported that used its close cousin, DMN. Recently, we showed some striking differences in the mutagenicity of DMN in fish versus rats.[21] Thus, in the present study, we sought to determine the stepwise differences in hepatic histomorphology between Japanese medaka (*Oryzias latipes*) and that published for Fisher 344 rats after exposure to DMN.

Small fish models are becoming commonplace in the laboratory and have been used for decades in chemical toxicity and carcinogenicity testing.[1,18,26,27,28] Fish can serve as environmental indicators as well as surrogates for human health problems and also have low husbandry costs and mature quickly, facilitating production of large numbers of fairly uniform animals for a given study. Small fish species such as the well-characterized Japanese medaka are sensitive to a wide variety of chemical carcinogens with a short time to tumorigenesis but have a low incidence of spontaneous neoplasia.[18,26,27,28,33] Use of small fish models has increased as pressures to find alternatives to current in vivo rodent models have grown. But how do we apply risk assessment data across such divergent phyletic levels as fish and rats, much less fish

[1] Integrated Laboratory Systems, Research Triangle Park, NC
[2] US Environmental Protection Agency, National Health & Environmental Effects Research Laboratory, Research Triangle Park, NC
[3] Department of Population Health and Pathobiology and Center for Comparative Medicine and Translational Research, College of Veterinary Medicine, North Carolina State University, Raleigh, NC

**Corresponding Author:**
Mac Law, Department of Population Health and Pathobiology, College of Veterinary Medicine, North Carolina State University, 4700 Hillsborough Street, Raleigh, NC 27606
Email: mac_law@ncsu.edu

and humans? Demonstration of common disease mechanisms, such as chemically induced biochemical alterations, can facilitate such interspecies extrapolations.

In a previous study, we sought to determine a ''molecular equivalent dose'' for aqueous DMN exposure between the F344 rat and the medaka fish model, using DNA adducts and mutant frequencies as surrogates for internal dose.[21] Although DNA adduct levels were comparable between medaka fish and rats, mutation induction was many-fold higher in medaka, suggesting a greater capacity for fish to convert DMN-induced DNA adducts to mutations. Presumably, differences at the molecular level such as mutation induction would show downstream, phenotypic effects in histomorphology.

Nitrosamines can be considered archetypal carcinogens, and DMN is a well-established model carcinogen in rodents. Tumors associated with DMN exposure involve the liver, lung, kidney, and nasal cavity.[43] Liver tumors are the most commonly observed neoplasms, with hepatocellular carcinomas (HCCs) the predominant phenotype.[35] DMN is also used in a rodent model of human alcoholic cirrhosis.[12,13] Patterns of DMN-induced liver injury and subsequent repair in the rat liver are similar to those described in humans with alcohol-induced liver disease.[12,19] In the few fish studies that used DMN, liver tumors also predominated. Rainbow trout and guppies had hepatocellular carcinomas, and individual tumor phenotypes of the liver were similar to those observed in rodents.[14,24] Behavioral changes in zebrafish and guppies exposed to DMN have been associated with DMN-induced hepatic injury; however, information regarding biochemical alterations associated with DMN-induced hepatic injury in fish is not known.

Transforming growth factor (TGF)-β1 is the predominant profibrogenic stimulus in DMN-induced fibrosis in the rat and in alcoholic cirrhosis in humans.[7] Mediation of the fibrogenic response occurs via TGF-β1's cell-signaling protein, Smad-3. Hepatocellular injury induces transdifferentiation of hepatic stellate cells (HSCs) to type-I collagen–producing myofibroblast-like cells (activated HSCs). TGF-β1 stimulates extracellular matrix (type-1 collagen) production by the activated hepatic stellate cells. These biochemical events lead to either hepatic repair and lesion resolution or perpetuation of collagenous matrix deposition and cirrhosis.[2,11] In addition to its profibrogenic activity, TGF-β1 effects DMN-induced injury via proliferative and growth-inhibition activities. TGF-β1 has the potential to function both as a tumor suppressor and as a tumor promoter.[9] In humans, cirrhosis often progresses to HCCs, and these neoplasms frequently display higher levels of TGF-β1 mRNA and protein than found in normal liver.[38] Both TGF-β1 and Smad-3 have been cloned from fish tissues.[8,16] However, the roles that TGF-β1 and Smad-3 play in DMN-induced injury, repair, and carcinogenesis in fish are unknown. Thus, in the present study, we sought to characterize DMN-induced hepatic injury and carcinogenesis in medaka fish and determine whether lesions occur via similar biochemical alterations to that reported for DMN-exposed rats.

## Materials and Methods

### Chemicals

Dimethylnitrosamine (DMN, $C_2H_6N_2O$; 99.9%, CAS 62-75-9, MW 74.08 g/mol) was purchased from Sigma-Aldrich (St. Louis, MO), and stored in a brown bottle sealed within a metal container at 4°C. All other chemicals and reagents used throughout the DMN experiments were of the highest purity available from commercial resources.

### Animals

Three-month-old Japanese medaka (*Oryzias latipes*) were used. Male and female, orange-red medaka (outbred, laboratory strain) were obtained from laboratory stocks at Duke University (kind gift from Dr. David Hinton) and Aquatic Research Organisms (Hampton, NH). Male and female, λ transgenic medaka were obtained from in-house populations at the Aquatic Biotechnology and Environmental Laboratory (ABEL), University of Georgia (Athens, GA). These λ transgenic fish were included in the study to determine whether any differences in hepatic response were induced by DMN. Medaka were acclimated for 2 weeks in reconstituted (1 g/liter Instant Ocean salts) reverse osmosis–purified (RO) water within a recirculating, freshwater culture system under an artificial light photoperiod (16 hours light/8 hours dark) at a temperature of 26°C ± 0.5°C. Animal care and use were in conformity with protocols approved by the Institutional Animal Care and Use Committee in accordance with the National Academy of Sciences Guide for the Care and Use of Laboratory Animals.

### Medaka DMN Exposures

Three groups of medaka were exposed to DMN in the ambient water. The first group consisted of 100 orange-red medaka and 50 λ transgenic medaka, the second of 110 orange-red medaka, and the third of 60 orange-red medaka included in a DNA adduct experiment (see Hobbie et al.[21]). All fish were exposed in 4-liter glass beakers containing 3 liters of reconstituted RO water at 1 g/liter salt concentration. For all exposures, medaka were randomly distributed among 4-liter glass beakers, 10–12 fish per beaker. Transgenic and nontransgenic medaka were exposed to DMN, separately, during the first exposure. Treatment beakers were placed within a recirculating, heated water bath to maintain temperature at 26°C ± 0.5°C throughout the exposures. The first group of medaka were exposed to 0, 10, 50, 100, or 200 μl/liter (ppm) DMN twice weekly for 4 weeks (Table 1). Because of increased mortality in the 200 ppm DMN group, the second and third exposure groups were exposed to 0, 10, 25, 50, or 100 ppm DMN twice weekly for 2 weeks. DMN was replaced every 3–4 days to allow for photodegradation of the compound (S. Revskoy, personal communication).[31] DMN dilutions were made from 1.5 liters of a 1000 ppm DMN stock solution prepared new prior to each treatment. Water quality was maintained with 50% water changes prior to each DMN treatment; ammonia levels remained within safe limits, always

**Table 1.** Dimethylnitrosamine (DMN) Exposure Protocol in Japanese Medaka Fish

| Medaka Exposure | Medaka Strain | No. of Fish | Experiment | DMN Doses, ppm | Exposure Length, wk | Grow-Out Period, mo | Sacrifices, n |
|---|---|---|---|---|---|---|---|
| 1 | *cII* transgenic | 50 | Pathology | 0, 10, 50, 100, 200 | 4 | 6 | 3 |
| 1 | Orange-red | 100 | Pathology | 0, 10, 50, 100, 200 | 4 | 6 | 3 |
| 2 | Orange-red | 110 | Pathology | 0, 10, 25, 50, 100 | 2 | 6 | 3 |
| 3 | Orange-red | 60 | Adduct Isolation | 0, 10, 25, 50, 100 | 2 | 6 | 1 |

less than 0.25 mg/liter. Fish were fed once daily with Aquatox Flake fish food (Zeigler Brothers, Gardners, PA). Animals were observed twice daily for physiological and behavioral responses and signs of overt toxicity. Following the 4-week and 2-week exposures, fish were removed from the treatment beakers, gently rinsed in clean water, and replaced into the recirculating, freshwater culture system for up to 6 months.

### *Sampling Method*

Subsets of medaka were euthanized with an overdose of tricaine methanesulfonate (300 mg/liter; MS-222, Argent Laboratories, Redmond, WA) intermittently throughout the 6-month grow-out period (Table 1), except for the third exposure group in which all fish were euthanized 1 month post exposure. The coelom of each fish was opened along the ventral midline to enhance fixation, and organs were examined macroscopically. Specimens were fixed in 10% neutral buffered formalin for 48 hours, demineralized in 10% formic acid for 24 hours, and transferred to 70% ethanol.

### *Tissue Processing and Histopathology*

All tissues were processed using standard histological techniques. Fish were embedded left side down in paraffin, sectioned at 5 μm, and stained with hematoxylin and eosin (HE). Internal organs and tissues of medaka were examined microscopically in multiple paramedian and midsagittal sections, with particular emphasis placed on the liver.

### *Histochemistry and Immunohistochemistry*

Additional paraffin sections from fish (3 per treatment group) were examined via histochemical and immunohistochemical methods. Five-micrometer sections of the fish were stained with histochemical stains Sirius red, Masson's trichrome, and reticulin. Primary antibodies used for immunohistochemistry in fish included cytokeratin (AE1/AE3), α-smooth muscle actin (α-SMA), muscle-specific actin (MSA), glial fibrillary acid protein (GFAP), factor VIII, transforming growth factor (TGF)-β1, and Smad-3 (TGF-β1 signaling protein). Cytokeratin, α-SMA, MSA, GFAP, and factor VIII stains were prepared with the Ventana automated stainer (Ventana Medical Systems, Tucson, AZ). An indirect immunoperoxidase method was used to stain with factor VIII (Dako, Carpinteria, CA), TGF-β1 (Santa Cruz, Santa Cruz, CA), and Smad-3 (Abcam, Cambridge, MA) antibodies. Biotinylated goat anti-rabbit and/or biotinylated goat anti-mouse immunoglobulin G was used as the secondary antibody. Deparaffinized tissue sections were treated with 3% hydrogen peroxide for 10 minutes to block endogenous peroxidases, and goat serum was used for 20 minutes to prevent nonspecific binding of the secondary antibody. Tissues were incubated with primary antibodies for 30 minutes, rinsed in phosphate-buffered saline (PBS), and then incubated with the secondary antibody for 20 minutes. Tissue sections were then treated for 20 minutes with streptavidin peroxidase. Visualization was achieved by treatment of tissue with liquid 3,3-diaminobenzidine (DAB) chromagen for 30–120 seconds, which in the presence of peroxidase produces a brown precipitate insoluble in alcohol. Slides were then rinsed in water, counterstained with Mayer's hematoxylin for 20–40 seconds, and dehydrated with xylene.

## Results

### *Histomorphologic Findings*

In total, 220 fish from the 3 exposures were examined microscopically for treatment-related lesions (Table 1). During the first exposure, approximately 25% of the total number of fish had died by the end of the 4-week exposure period, of which 53% of those deaths occurred in the 200 ppm DMN group. Exclusion of the 200 ppm DMN exposure group and readjustment of the exposure period to 2 weeks decreased the total number of exposure-related deaths to 5% in the second exposure and 0% in the third exposure.

Microscopically, 100% of orange-red medaka exposed to 100 ppm DMN 30 days post exposure had necrotic livers. This finding was consistent with the small, pale, and friable livers seen in λ transgenic medaka exposed to 100 ppm DMN for 2 weeks. No differences were noted in the numbers of exposure-related deaths or DMN-induced changes for transgenic versus nontransgenic medaka.

No remarkable microscopic abnormalities were seen in tissues other than the liver in medaka. Liver lesions of DMN-exposed medaka were identified and described based on criteria set by the National Toxicology Program.[3] Degenerative and nonneoplastic proliferative changes of the liver were the most prevalent lesions, with neoplasms occurring less often. Liver lesions had similar morphology among the 3 exposure groups (Table 2). The overall incidence and severity of many lesions increased with higher DMN exposure levels for all 3 exposures. Livers from fish exposed to 10 ppm DMN for 4 weeks (exposure 1) were histologically normal until the third

**Table 2.** Degenerative and Proliferative Hepatic Lesions in Medaka at Each Dimethylnitrosamine Exposure and Sacrifice

| Group/Dose/ Days PE[a] | Cellular Degeneration | Necrosis/ Apoptosis | Architectural Change | BPDEC Proliferation | Stellate Cells ↑ | Bile Duct Hyperplasia | Fibrosis/Spindle Cells ↑ | Cellular Dysplasia | Liver Regeneration |
|---|---|---|---|---|---|---|---|---|---|
| I/200/30 | 3/6 | 6/6 | 6/6 | 4/6 | 4/6 | 4/6 | 2/6 | 1/6 | 0/6 |
| I/100/30 | 6/10 | 6/10 | 6/10 | 7/10 | 6/10 | 5/10 | 2/10 | 2/10 | 0/10 |
| I/50/30 | 3/8 | 0/8 | 1/8 | 1/8 | 1/8 | 3/8 | 1/8 | 1/8 | 0/8 |
| I/10/30 | 0/8 | 0/8 | 0/8 | 0/8 | 0/8 | 0/8 | 0/8 | 0/8 | 0/8 |
| I/0/30 | 0/9 | 0/9 | 0/9 | 0/9 | 0/9 | 0/9 | 0/9 | 0/9 | 0/9 |
| I/200/90 | 0/0 | 0/0 | 0/0 | 0/0 | 0/0 | 0/0 | 0/0 | 0/0 | 0/0 |
| I/100/90 | 4/6 | 5/6 | 3/6 | 2/6 | 1/6 | 4/6 | 3/6 | 2/6 | 0/6 |
| I/50/90 | 5/9 | 5/9 | 3/9 | 1/9 | 1/9 | 2/9 | 3/9 | 2/9 | 1/9 |
| I/10/90 | 0/8 | 0/8 | 0/8 | 0/8 | 0/8 | 0/8 | 0/8 | 0/8 | 0/8 |
| I/0/90 | 0/9 | 0/9 | 0/9 | 0/9 | 0/9 | 0/9 | 0/9 | 0/9 | 0/9 |
| I/200/150 | 0/0 | 0/0 | 0/0 | 0/0 | 0/0 | 0/0 | 0/0 | 0/0 | 0/0 |
| I/100/150 | 3/3 | 2/3 | 3/3 | 0/3 | 0/3 | 0/3 | 1/3 | 1/3 | 3/3 |
| I/50/150 | 7/10 | 5/10 | 3/10 | 2/10 | 1/10 | 3/10 | 1/10 | 3/10 | 2/10 |
| I/10/150 | 3/9 | 0/9 | 0/9 | 0/9 | 0/9 | 3/9 | 0/9 | 0/9 | 1/9 |
| I/0/150 | 1/10 | 0/10 | 0/10 | 0/10 | 0/10 | 2/10 | 0/10 | 0/10 | 0/10 |
| II/100/60 | 4/4 | 3/4 | 3/4 | 3/4 | 2/4 | 2/4 | 2/4 | 2/4 | 2/4 |
| II/50/60 | 3/4 | 2/4 | 1/4 | 0/4 | 0/4 | 1/4 | 1/4 | 0/4 | 0/4 |
| II/25/60 | 3/6 | 2/6 | 1/6 | 0/6 | 0/6 | 0/6 | 0/6 | 1/6 | 0/6 |
| II/10/60 | 2/6 | 1/6 | 0/6 | 0/6 | 0/6 | 0/6 | 0/6 | 0/6 | 0/6 |
| II/0/60 | 1/5 | 0/5 | 0/5 | 0/5 | 0/5 | 0/5 | 0/5 | 0/5 | 0/5 |
| II/100/120 | 2/2 | 1/2 | 2/2 | 1/2 | 1/2 | 1/2 | 2/2 | 2/2 | 0/2 |
| II/50/120 | 4/4 | 2/4 | 2/4 | 0/4 | 0/4 | 1/4 | 1/4 | 1/4 | 0/4 |
| II/25/120 | 2/5 | 0/5 | 1/5 | 0/5 | 0/5 | 0/5 | 0/5 | 0/5 | 0/5 |
| II/10/120 | 0/4 | 0/4 | 0/4 | 0/4 | 0/4 | 0/4 | 0/4 | 0/4 | 0/4 |
| II/0/120 | 1/5 | 0/5 | 0/5 | 0/5 | 0/5 | 0/5 | 0/5 | 0/5 | 0/5 |
| II/100/180 | 4/4 | 3/4 | 2/4 | 2/4 | 1/4 | 3/4 | 2/4 | 0/4 | 0/4 |
| II/50/180 | 3/4 | 2/4 | 3/4 | 2/4 | 1/4 | 1/4 | 2/4 | 1/4 | 0/4 |
| II/25/180 | 4/5 | 3/5 | 1/5 | 1/5 | 0/5 | 2/5 | 1/5 | 1/5 | 0/5 |
| II/10/180 | 2/4 | 0/4 | 0/4 | 0/4 | 0/4 | 1/4 | 0/4 | 0/4 | 0/4 |
| II/0/180 | 0/6 | 0/6 | 0/6 | 0/6 | 0/6 | 0/6 | 0/6 | 0/6 | 0/6 |
| III/100/30 | 4/5 | 5/5 | 5/5 | 5/5 | 5/5 | 4/5 | 3/5 | 5/5 | 1/5 |
| III/50/30 | 8/10 | 4/10 | 10/10 | 10/10 | 8/10 | 6/10 | 9/10 | 8/10 | 3/10 |
| III/25/30 | 5/12 | 1/12 | 2/12 | 3/12 | 2/12 | 3/12 | 1/12 | 0/12 | 0/12 |
| III/10/30 | 6/12 | 0/12 | 0/12 | 1/12 | 0/12 | 1/12 | 0/12 | 0/12 | 0/12 |
| III/0/30 | 1/8 | 0/8 | 0/8 | 0/8 | 0/8 | 0/8 | 0/8 | 0/8 | 0/8 |

BPDEC, bile preductular epithelial cell.
[a] Group (exposure groups I, II, III)/dose (ppm dimethylnitrosamine)/days post exposure.

sacrifice, when degenerative changes became apparent. Some degree of cellular degeneration was apparent at all dose levels and time periods in fish exposed to DMN for 2 weeks (exposures 2 and 3), although the severity increased with higher DMN doses. A greater percentage of DMN-induced neoplasms occurred in the second exposure group (13/68 fish) compared with the first exposure group (6/105 fish); no neoplasms were present in the third exposure group.

Normal livers from medaka controls are depicted in Figs. 1 and 2. The principle nonneoplastic microscopic lesions in the livers of DMN-exposed medaka are illustrated in Figs. 3–11. Degenerative changes in the liver included glycogen loss, hyalinization of hepatocyte cytoplasm, vacuolation of hepatocyte cytoplasm, hepatocellular apoptosis and necrosis, cystic degeneration (spongiosis hepatis), and hepatic cysts. Proliferative changes of the liver included hyperplasia of bile ducts, bile preductular epithelial cells (BPDECs), and HSCs; spindle cell hyperplasia with collagen matrix deposition; and foci of cellular alteration (altered foci).

Degenerative changes of the liver in DMN-exposed medaka were characterized by generalized glycogen depletion of hepatocytes (Fig. 3), individual and/or clusters of swollen hepatocytes with vacuolated or glassy, hypereosinophilic cytoplasm (Figs. 4, 5), and cellular dropout. With lesion progression, swelling and hyalinization of hepatocytes became more diffuse, with loss of the normal hepatic cords and collapse of sinusoids (Fig. 6). Degenerate hepatocytes were often distended by variably sized, hypereosinophilic, intracytoplasmic globules. Degenerative changes were variably accompanied by chronic inflammatory infiltrates, predominantly lymphocytes and macrophages. Multifocal regions of necrotic liver were replaced by multiloculated cyst-like structures (cystic degeneration) often composed of a meshwork of interconnected perisinusoidal cells (HSCs) and/or flocculent

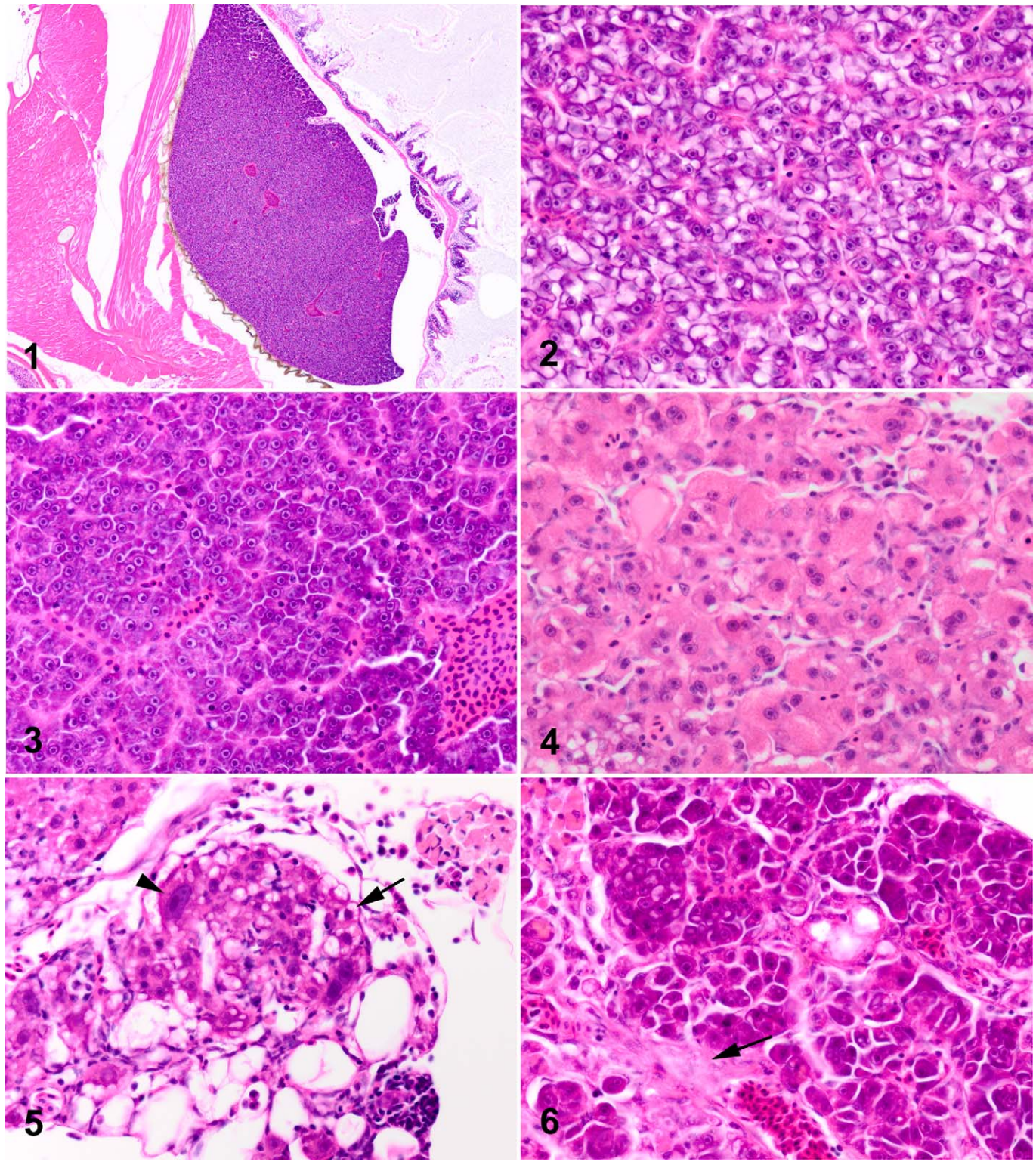


**Figure 1.** Normal liver, control medaka (0 ppm dimethylnitrosamine [DMN]) at 2 months post exposure (PE) (20×). **Figure 2.** Control medaka liver, 2 months PE (400×). Higher magnification of normal hepatic parenchyma. Note clear intracytoplasmic vacuoles (arrows) within hepatocytes (presumed glycogen and/or lipid). **Figure 3.** Medaka liver, 10 ppm DMN at 6 months PE (400×). Note depeletion of normal glycogen and/or lipid stores. **Figure 4**. Medaka liver, 50 ppm DMN at 6 months PE (600×). Note cell swelling and hyalinization of hepatocyte cytoplasm. **Figure 5**. Medaka liver, 100 ppm DMN at 4 months PE (600×). Note hepatocyte swelling, cytoplasmic vacuolization (arrow), and cytomegaly (arrowhead). The reticular framework is retained as individual hepatocytes are lost (600×). **Figure 6**. Medaka liver, 50 ppm DMN at 4 months PE (400×). Note increased pericellular extracellular matrix (collagen) deposition (arrow).

eosinophilic material (Fig. 7). Hepatic cysts, characterized by clear cavities lined by hepatocytes, were less common. Inflammation was occasionally associated with cystic degeneration of the liver and/or hepatic cysts. With progressive loss of the hepatic parenchyma, BPDECs (purported liver stem cells) and intermediate cells (immature bile duct epithelial cell and/or hepatocytes) proliferated, infiltrating along hepatic plates (Fig. 8), often forming small basophilic tubules (bile ducts and/or regenerative hepatocytes). Proliferating HSCs and/or BPDECs surrounded and ''individualized'' hepatocytes (satellitosis), giving affected portions of the liver a fenestrated appearance (Fig. 9). As hepatic degeneration became more chronic, multifocal spindle cells (possible myofibroblasts or cells of biliary origin) dissected the hepatic parenchyma, accompanied by bundles of pale, eosinophilic fibrillar matrix (presumed collagen). Often, only this matrix was apparent as fine, pale, eosinophilic fibrillar tendrils multifocally infiltrating between and around hepatocytes (Fig. 6). In addition, proliferation of fibrous connective tissue was associated with localized hyperplasia of bile ducts. In some medaka, hepatocytes became dysplastic, increasing dramatically in size with bizarre euchromatic nuclei and large magenta nucleoli (Figs. 5, 9). Dysplastic hepatocytes were often multinucleated with multiple, variably sized nucleoli. As described by Okihiro and Hinton,[33] ''nodular proliferations'' of hepatocytes, characterized by distinct borders, loss of the normal hepatic architecture, and megalocytosis and pleomorphism of affected hepatocytes, were present. With progressive hepatotoxicity, cirrhotic-like nodules characterized by nodular accumulations of degenerate hepatocytes surrounded by spindle cells and collagenous connective tissue became more apparent (Fig. 10). Eventually, the hepatic architecture changed remarkably, becoming multinodular, as significant portions of liver were lost and replaced (Fig. 11). Regeneration of the liver was evident, in some fish, as nodular to diffuse replacement of the hepatic parenchyma by plump, densely basophilic and/or amphophilic (regenerative) hepatocytes.

Altered foci were apparent in DMN-exposed medaka within 90 days post exposure (Table 3). Eosinophilic foci were more prevalent than basophilic or clear cell foci (9/12 foci). All foci were small, discrete areas of normal hepatocytes, save for the distinct tinctorial change in their cytoplasm. Hepatocytes of clear cell foci had finely vacuolated, clear cytoplasm and centrally placed nuclei. Aside from their tinctorial demarcation, foci otherwise appeared to blend imperceptibly with the surrounding hepatic parenchyma.

The principle neoplastic lesions diagnosed in the livers of DMN-exposed medaka are illustrated in Figs. 12–17, which can be found in the online supplement: http://www.vet.sagepub.com/supplement. Neoplasms included hepatocellular carcinomas (solid, megalocytic, trabecular, and anaplastic variants), mixed carcinomas, and a cholangioma. Neoplasms seen in DMN-exposed fish were predominantly malignant and similar to those described for medaka exposed to DEN.[33] Hepatocellular carcinomas were the most common (12/19) neoplasm diagnosed in DMN-exposed medaka, with solid variants occurring much more often than megalocytic, trabecular, or anaplastic HCCs (Table 3). Mixed (hepatocellular and biliary) carcinomas were the second most prevalent hepatic tumors (6/19). One cholangioma was present. The cholangioma was a small, well-circumscribed, nonencapsulated mass that minimally compressed the adjacent hepatic parenchyma. It was composed of fairly well-differentiated bile duct epithelial cells that formed closely packed, tortuous ducts in a collagenous stroma.

As in Okihiro and Hinton,[33] the solid variant of HCC was characterized by replacement of the normal (muralium) hepatic architecture by diffuse, poorly demarcated sheets of neoplastic hepatocytes (Fig. 8). Neoplastic hepatocytes of solid HCCs were variable in size and shape with abundant amounts of pale, glassy, eosinophilic cytoplasm and indistinct cell borders. Nuclei were usually centrally located and had lacy chromatin with 1–2 magenta nucleoli. Quite often, neoplastic hepatocytes contained round, euchromatic nuclei with 1 large, centrally located nucleolus, giving neoplastic hepatocytes a ''fish-eye'' appearance. Multinucleated neoplastic hepatocytes were fairly common with mitoses variably present. Megalocytic HCCs differed from the solid variant in that neoplastic hepatocytes were markedly enlarged and pleomorphic, with karyomegalic nuclei (Fig. 12). Trabecular HCCs were characterized by mildly pleomorphic, amphophilic hepatocytes arranged as thick, irregular cords (>2 cells thick) that maintained the general hepatic architecture (Fig. 13; Note: Figures 13-32 can be found online. To view the online supplement, please to http://www.vet.sagepub.com/supplemental). Neoplastic cells of anaplastic HCCs were highly pleomorphic hepatocytes, varying from spindle to stellate or polygonal in shape (Fig. 14). Cellular margins of anaplastic hepatocytes were extremely indistinct and their arrangements were dense and haphazard. Phenotypic features of neoplastic hepatocytes quite often overlapped among the different variants of HCCs; HCC variant was diagnosed based upon the predominant neoplastic feature. Mixed carcinomas were composed of both neoplastic hepatocytes (Fig. 15) and biliary epithelial cells (Fig. 16). These tumors were poorly defined, often large, multinodular masses that replaced most or all of the liver. Neoplastic hepatocytes varied from fairly well-differentiated, amphophilic cells (similar to those of trabecular HCCs) to pleomorphic hepatocytes (akin to anaplastic HCCs) with spindle, stellate, or polygonal features. Groups of neoplastic hepatocytes would occasionally contain multiple, hypereosinophilic globules within their cytoplasm, similar to those described for degenerative hepatocytes (Fig. 15). The malignant biliary component was characterized by moderately pleomorphic, small to large cuboidal epithelial cells arranged as irregular ducts or highly pleomorphic, bizarre, angular epithelial cells that formed poorly defined, tortuous, and infiltrative tubules (Fig. 16). Neoplastic bile ducts were separated by variable amounts of fibrous stroma. In anaplastic mixed carcinomas, spindyloid hepatocytes and biliary epithelial cells were often difficult to distinguish from each other, blending imperceptibly. One mixed carcinoma was composed predominantly of finely tapered spindle cells (presumed biliary origin) arranged as densely packed, interweaving fascicles that entrapped multifocal, irregular islands of neoplastic hepatocytes (Fig. 17). In some neoplasms (HCCs and/or mixed), small cells with scant

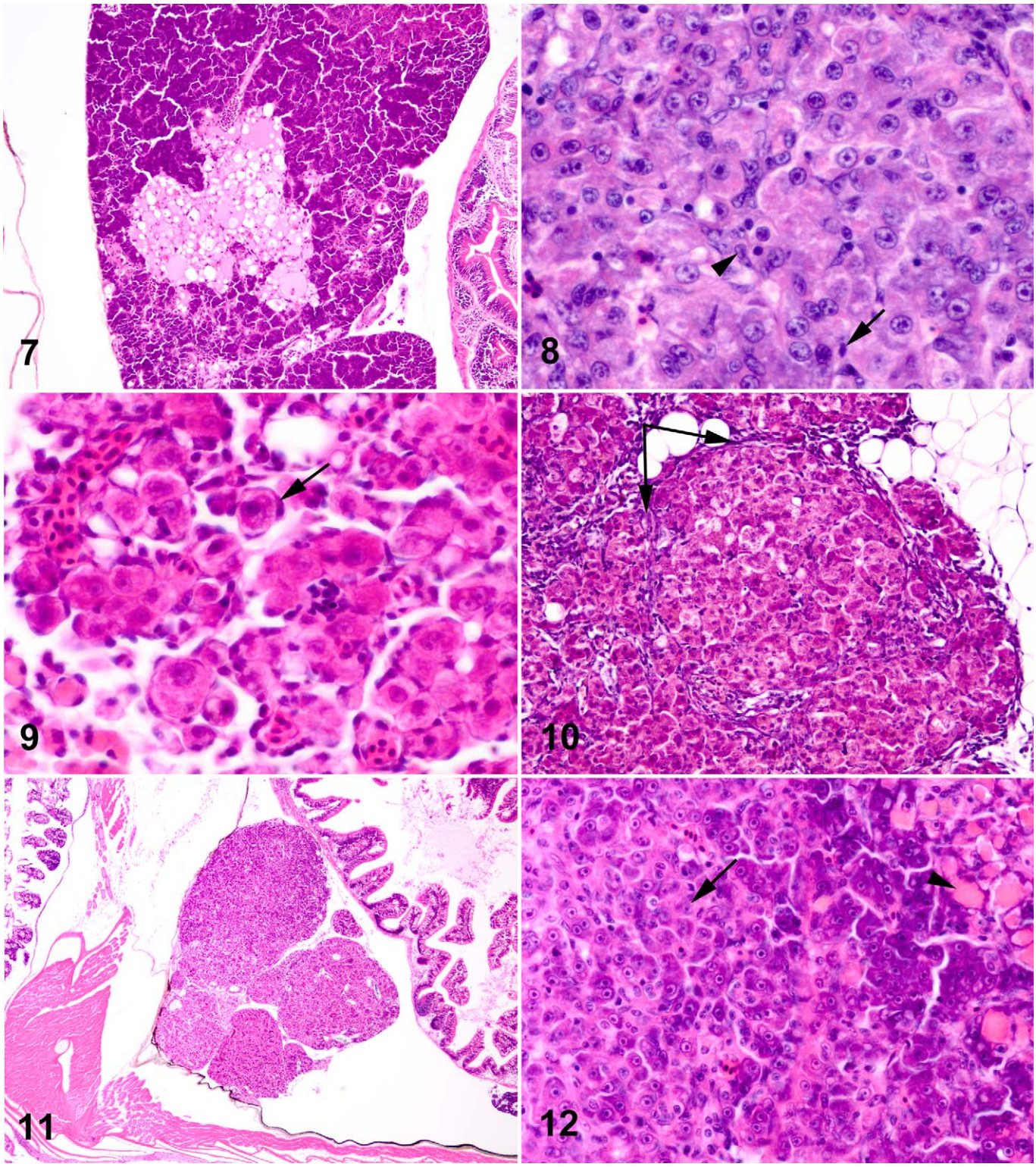


**Figure 7.** Medaka liver, 100 ppm dimethylnitrosamine (DMN) at 6 months post exposure (PE) (200×). Note cystic degeneration of liver composed of a multilocular meshwork of interconnected perisinusoidal cells (HSCs) and/or flocculent eosinophilic material. **Figure 8**. Medaka liver, 100 ppm DMN at 2 months PE (600×). Note perihepatocellular proliferation of small cells with scant cytoplasm and oval hyperchromatic nuclei consistent with bile preductular epithelial cells (BPDECs) (arrow). Slightly larger cells with oval euchromatic nuclei are presumably intermediate cells (arrowhead). **Figure 9**. Medaka liver, 100 ppm DMN at 2 months PE (600×). Note HSC and/or BPDEC proliferation and how the cells wrap around individual hepatocytes (arrow), giving a fenestrated appearance to the tissue. **Figure 10**. Medaka liver, 100 ppm DMN at 1 month PE (200×). Note cirrhotic-like nodule of regenerative hepatocytes bordered by BPDECs and fibrils of connective tissue (arrows).

**Table 3.** Hepatic Foci of Cellular Alteration and Neoplasms in Medaka at Each Dimethylnitrosamine Exposure and When Euthanatized

| Group/Dose/Days PE[a] | Foci of Cellular Alteration | Solid HCCs | Megalocytic HCCs | Trabecular HCCs | Anaplastic HCCs | Mixed Carcinoma | Cholangioma |
|---|---|---|---|---|---|---|---|
| I/200/30 | –[b] | – | – | – | – | – | – |
| I/100/30 | – | – | – | – | – | – | – |
| I/50/30 | – | – | – | – | – | – | – |
| I/10/30 | – | – | – | – | – | – | – |
| I/0/30 | – | – | – | – | – | – | – |
| I/200/90 | – | – | – | – | – | – | – |
| I/100/90 | 1/6 | – | – | – | – | – | – |
| I/50/90 | 1/9 | 2/9 | – | – | – | – | – |
| I/10/90 | – | – | – | – | – | – | – |
| I/0/90 | – | – | – | – | – | – | – |
| I/200/150 | – | – | – | – | – | – | – |
| I/100/150 | 1/3 | – | – | 1/3 | – | – | – |
| I/50/150 | 1/10 | 2/10 | – | – | – | 1/10 | – |
| 1/10/150 | – | – | – | – | – | – | – |
| I/0/150 | – | – | – | – | – | – | – |
| II/100/60 | – | – | – | – | – | – | – |
| II/50/60 | – | – | – | – | – | 1/4 | – |
| II/25/60 | – | – | – | – | – | – | – |
| II/10/60 | – | – | – | – | – | – | – |
| II/0/60 | – | – | – | – | – | – | – |
| II/100/120 | – | – | 1/2 | – | – | 1/2 | 1/2 |
| II/50/120 | 2/4 | 2/4 | – | – | – | – | – |
| II/25/120 | 1/5 | – | – | – | – | – | – |
| II/10/120 | – | – | – | – | – | – | – |
| II/0/120 | – | – | – | – | – | – | – |
| II/100/180 | – | 1/4 | – | – | – | 1/4 | – |
| II/50/180 | 1/4 | 1/4 | – | 1/4 | 1/4 | 1/4 | – |
| II/25/180 | 3/5 | – | 1/5 | – | – | 1/5 | – |
| II/10/180 | 1/4 | – | – | – | – | – | – |
| II/0/180 | – | – | – | – | – | – | – |
| III/100/30 | – | – | – | – | – | – | – |
| III/50/30 | – | – | – | – | – | – | – |
| III/25/30 | – | – | – | – | – | – | – |
| III/10/30 | – | – | – | – | – | – | – |
| III/0/30 | – | – | – | – | – | – | – |

HCC, hepatocellular carcinoma.
[a] Group (exposure groups I, II, III)/dose (ppm dimethylnitrosamine)/days post exposure.
[b] Dash indicates that lesion is not present.

eosinophilic cytoplasm and small, hyperchromatic nuclei (consistent with BPDECs) infiltrated "single-file" in and around neoplastic cells (Fig. 8). Occasionally, these cells would form small acini and thin, irregular ductules within the neoplasm. Usually, degenerative changes similar to those previously described were present in the hepatic parenchyma adjacent to HCCs and/or mixed carcinomas.

## *Histochemical and Immunohistochemical Findings*

Histochemical and immunohistochemical methods were used to further characterize DMN-induced degenerative, proliferative, and neoplastic changes in Japanese medaka and to determine potential mechanisms of action for these changes based on similar changes documented for DMN-exposed rodents. Histochemical and immunohistochemical stains used for these purposes included TGF-β1, Smad-3, cytokeratin, Sirius red, reticulin, α-SMA, MSA, factor VIII (Von Willebrand factor), and GFAP. Functions and cellular activities for these stains in livers of DMN-exposed medaka are presented in Tables 4 and 5. Medaka tissue sections were chosen for special staining based on dose and lesion. Specific lesions of interest included hepatocellular necrosis/apoptosis, alteration of the hepatic architecture, BPDEC proliferation, HSC hyperplasia, hepatocellular regeneration, spindle cell proliferation, fibrosis, cellular dysplasia (or foci of preneoplasia), and hepatic

**Figure (continued). Figure 11**. Medaka liver, 100 ppm DMN at 4 months PE (40×). Chronic hepatotoxicity with loss, collapse, and regeneration of the hepatic parenchyma resulting in a multinodular (or multilobulated) liver. **Figure 12**. Medaka liver, 25 ppm DMN at 6 months PE (400×). Solid version of hepatocellular carcinoma (arrow). Note degenerate hepatocytes with hypereosinophilic cytoplasm (arrowhead).

**Table 4.** Function and Cellular Activity (Normal and Treatment-Related) of Selected Histochemical and Immunohistochemical Stains in Dimethylnitrosamine-Exposed Medaka Fish

| Stain | Function | Normal Activity | Treatment-Related Activity |
|---|---|---|---|
| TGF-β1 | Reacts with 25-kD TGF-β1 protein. | BPDECs | BPDECs, intermediate cells, immature hepatocytes, hepatocytes |
| Smad-3 | Reacts with 50-kD Smad-3 protein. | Hepatocyte cytoplasm | Hepatocyte cytoplasm and nuclei (increased staining) |
| Cytokeratin AE1/AE3[a] | Recognizes high- and low-molecular-weight cytokeratins. | Bile duct epithelium | BPDECs and intermediate cells HSCs (?) |
| Sirius Red | Reacts with collagen. | Blood vessel walls | Pericellular fibrillar material (presumed collagen) |
| Reticulin | Reacts with reticular fibers (type III collagen). | Blood vessel wall basement membrane | Pericellular staining increased, new basement membranes |
| MSA | Reacts with 42-kD protein specific for actins in skeletal, cardiac, and smooth muscle. | Periductal myofibroblasts | Pericellular staining (presumed activated HSCs); also periductal myofibroblasts |
| GFAP | Reacts with class II intermediate filament protein. | Astrocytes/astroglia | None |

BPDEC, bile preductular epithelial cell; GFAP, glial fibrillary acidic protein; HSC, hepatic stellate cell; MSA, muscle-specific actin; Smad-3, mammalian homologs of the Drosophila Mothers against dpp (Mad) and *Caenorhabditis elegans* (Sma); TGF-β1, transforming growth factor-β1.
[a] AE1 recognizes 10,14, 15, 16, and 19; AE3 recognizes 1, 2, 3, 4, 5, 6, and 8.

**Table 5.** Results of Histochemical and Immunohistochemical Staining in Livers of Medaka Exposed to Dimethylnitrosamine (DMN)

| DMN, ppm | TGF-β1 | SMAD3 | Cytokeratin | Sirius Red | Reticulin | α-SMA | MSA | Factor VIII | GFAP |
|---|---|---|---|---|---|---|---|---|---|
| 200 | 3/3 [2–3+][a] | 3/3 [2–3+] | 3/3 [3–4+] | 3/3 [2–3+] | 3/3 [2–3+] | –[b] | 3/3 [1+] | – | 0/3 |
| 100 | 2/3 [1–4+] | 3/3 [3–4+] | 3/3 [2–4+] | 3/3 [1–3+] | 3/3 [1–3+] | – | 3/3 [1–2+] | – | 0/3 |
| 50 | 3/3 [2–4+] | 2/3 [2+] | 2/3 [2–4+] | 3/3 [1–3+] | 3/3 [2–4+] | – | 2/3 [1–2+] | – | 0/3 |
| 25 | 3/3 [1+] | 1/3 [1+] | 1/3 [1+] | 0/3 | 2/3 [1+] | – | 0/3 | – | 0/3 |
| 10 | 3/3 [1+] | 0/3 | 2/3 [1+] | 0/3 | 0/3 | – | 0/3 | – | 0/3 |
| 0 | 0/3 | 0/3 | 0/3 | 0/3 | 0/3 | – | 0/3 | – | 0/3 |

α-SMAD3α-smooth muscle actin; GFAP, glial fibrillary acidic protein; MSA, muscle-specific actin; TGF-β1, transforming growth factor-β1.
[a] + (minimal), 2+ (mild), 3+(moderate), and 4+(marked) increase in staining.
[b] Dash indicates that the stain did not work on medaka tissue.

neoplasms. Preliminary staining of medaka tissue with factor VIII and α-SMA proved unsuccessful; medaka tissue sections stained only with TGF-β1, Smad-3, cytokeratin, Sirius red, reticulin, MSA, and GFAP stains. The relative magnitudes of histochemical and immunohistochemical staining in livers of DMN-exposed medaka are summarized in Table 5.

Staining of liver tissue for TGF-β1, Smad-3, cytokeratin, Sirius red, reticulin, and MSA in control fish is illustrated in Figs. 18–23. In control fish, faint (1+), positive staining with TGF-β1 was limited to the cytoplasm of multifocal BPDECs positioned at the interface of hepatocytes and intrahepatic biliary passageways (IHBPs; also bile canaliculi) (Fig. 18). Faint (1+) staining with Smad-3 was evident in cytoplasm of hepatocytes directly adjacent to IHBPs (Fig. 19). The cytoplasm of bile ducts and BPDECs stained positively (1+) with cytokeratin (Fig. 20). The collagen in blood vessel walls of control medaka stained positively (2+) with the Sirius red stain (Fig. 21). Myofibroblasts along the perimeter of occasional bile ductules stained positively (1+) with the MSA stain; otherwise, medaka livers stained negatively for MSA (Fig. 22). The basement membranes of multifocal, large blood vessels and small arterioles stained intensely with the reticulin stain (Fig. 23). The livers of control medaka did not stain with GFAP; however, positive GFAP staining was apparent in the brain and spinal cord of the control fish.

Staining for TGF-β1, Smad-3, cytokeratin, Sirius red, reticulin, and MSA in livers of DMN-treated fish is illustrated in Figs. 24–32. Increased staining with TGF-β1 (1+ to 4+) was evident in all DMN-treated medaka (Table 5). Positive TGF-β1 staining increased with increasing DMN exposure, although subjectively there was little staining variation between medaka in the 50, 100, and 200 ppm DMN groups. As in control medaka, BPDECs of treated fish stained for TGF-β1, although the number of BPDECs affected was often markedly increased (Fig. 24). In addition, many intermediate cells, immature hepatocytes, and fewer mature hepatocytes stained for TGF-β1, particularly in DMN-treated medaka with degenerative lesions; cells with similar morphologic features present within hepatic neoplasms also stained for TGF-β1 (Fig. 25). Dysplastic hepatocytes tended to stain consistently for TGF-β1, whereas TGF-β1 staining of neoplastic cells was occasionally decreased. Negative staining of neoplastic cells for TGF-β1 often correlated with negative staining of the same cells for Smad-3 (TGF-β1's cell-signaling protein). Sometimes, neoplastic cells stained for TGF-β1 but stained negatively for Smad-3, whereas other neoplasms stained for both TGF-β1 and

Smad-3 (Figs. 25, 26). Overall, positive staining with Smad-3 was less distinct and characterized by patchy, cell-specific increases in the amount and intensity of cytoplasmic staining for Smad-3. Occasionally, individual cells demonstrated nuclear staining for Smad-3. Regions of increased Smad-3 staining in DMN-treated fish usually correlated with the general distribution of increased TGF-β1 staining. Increased Smad-3 staining occurred in all DMN treatment groups, except for fish exposed to 10 ppm DMN. Like TGF-β1, staining for cytokeratin was apparent in all treated medaka, although the intensity and amount of staining were greater in the 50, 100, and 200 ppm DMN exposure groups. Increased cytokeratin staining usually correlated with increased numbers of BPDECs and intermediate cells present within the affected liver sections (Fig. 27). BPDECs and intermediate cells that stained for cytokeratin often stained for TGF-β1 as well (Fig. 24). The pale, eosinophilic fibrillar material (presumptive collagen) seen on HE stain in livers of treated medaka stained positively with the Sirius red histochemical stain (Fig. 28). Pericellular material surrounding degenerative hepatocytes often stained positively for Sirius red (Fig. 29). Staining of the fibrillar material with Sirius red was generally fainter than the staining of collagenous blood vessel walls by the same stain. Sometimes this correlated with positive staining with cytokeratin (Fig. 30). Staining for Sirius red was increased only in medaka treated with 50, 100, and 200 ppm DMN. Reticulin staining was increased in livers of medaka evaluated from the 25, 50, 100, and 200 ppm DMN groups. Increased reticular staining was often associated with marked structural changes in the liver, the reticulin stain highlighting a complex pattern of multifocally branching basement membranes (Fig. 31). Rare perisinusoidal cells (presumed HSCs) and bile ductule myofibroblasts stained faintly positive (1–2+) with MSA in fish exposed to 50, 100, and 200 ppm DMN (Fig. 32). Occasionally, MSA staining of perisinusoidal cells was accompanied by focal deposition of fibrillar matrix material in the within the hepatic parenchyma. Positive staining of HSCs with GFAP was not present in any of the livers examined from DMN-treated medaka.

## Discussion

Small fish models, as bioindicators of environmental health, can provide valuable scientific insight into potential environmental hazards to human health. Their advantage in numbers, sensitivity to a variety of known carcinogens, and low spontaneous tumor rate make them an ideal alternative to traditional rodent carcinogenicity assays, particularly with regard to low-dose chemical exposures.[18,26,27,28,33] However, more comparative data across phyletic levels are necessary to validate the use of fish as models for specific human diseases. Because pathology involves more than what is observed at the tissue level, determining common mechanisms for particular lesions should help to determine whether a particular fish model is appropriate for a specific human disease. However, few comparative data exist for fish and rats, much less for fish and humans.

In a previous study, we attempted to determine a molecular equivalent dose for aqueous nitrosamine exposure between 2 commonly used laboratory animals, the F344 rat and the medaka fish.[21] Using DMN-induced DNA adducts and mutant frequencies as surrogates for internal dose, we attempted to make dose comparisons between the 2 species by using fold differences in apparent compound potency at the common molecular level. We found that mutant frequencies were magnitudes higher for DMN-exposed medaka versus rat when compared with adduct levels in both animals, suggesting an increased capability of medaka to convert DMN adducts to mutations. The purpose of our current study was to compare DMN-induced lesions between medaka fish and F344 rats and determine any common disease mechanisms that would improve interspecies comparisons.

DMN-induced hepatic neoplasia is a well-established model in rodents. DMN-exposure in rodents is associated with tumors of the liver, lung, kidney, and nasal cavity.[43] In a lifetime study, liver tumors (hepatocellular, bile duct, blood vessels, and Kupffer cells) were the most commonly observed neoplasms in DMN-exposed rats.[35] Of the different liver tumors described in that study, HCCs predominated. DMN-induced liver injury is also a good and reproducible experimental system for studying biochemical and pathophysiological alterations associated with the development of hepatic fibrosis and cirrhosis in human beings.[12,13] The changes of DMN-induced fibrosis in rats are reported to include massive centrilobular hepatocellular necrosis, collapse of the liver parenchyma, congestion and hemorrhage, fibrillar (collagenous) septa formation, cirrhotic nodules, hepatocellular regeneration, and specific biochemical abnormalities.[12,19]

DMN is also a model carcinogen in fish. DMN-induced tumors have been documented in zebrafish (*Danio rerio*), guppies (*Poecilia reticulata*), and rainbow trout (*Salmo gairdneri*). Most of the neoplasms reported in DMN-exposed fish were hepatocellular in origin, with cholangiocellular tumors occurring less frequently.[14,24] Khudoley[24] reported hepatocellular necrosis and rearrangement of the hepatic architecture associated with behavioral changes in DMN-exposed zebrafish and guppies; however, more detailed data on DMN-induced hepatic injury in fish have not been reported until now.

To compare the progression of DMN-induced hepatic injury and carcinogenesis in medaka fish with that reported for DMN-exposed rats and to determine possible common DMN-induced biochemical and pathophysiological alterations between the 2 species, medaka fish were exposed to various DMN concentrations in their ambient water for 2 or 4 weeks and intermittently euthanatized over a period of 6 months. Depending on the desired endpoint, DMN exposure protocols designed for rats include intraperitoneal injections of DMN for 3 days to induce hepatic fibrosis and lengthy drinking water exposures (1–1.5 years) to induce carcinogenesis. A species-specific difference in the effective DMN dose and time to effect was a challenge in directly comparing DMN-induced lesions of medaka and rats. However, the effects of DMN on the liver

of the rat are already well established, so although data from a parallel DMN exposure using F-344 rats would have been ideal, it was not necessary to induce DMN-associated lesions in rats. Neoplasms occurred much less frequently in DMN-exposed medaka than did degenerative lesions in DMN-exposed medaka. However, the specific types of neoplasms (hepatocellular and/or biliary origin) were consistent with those reported for rats exposed at length to DMN in their drinking water. Similar to the findings of Peto et al.,[35] the predominant hepatic neoplasms in DMN-exposed medaka were hepatocellular carcinomas. However, unlike the rat, neoplasms involving other tissues, such as kidney, were not found in medaka exposed to DMN. More neoplasms were noted in medaka exposed to DMN for 2 weeks versus medaka exposed to DMN for 4 weeks. Cutroneo et al.[6] noted that excessive fibrosis and formation of benign tumors were associated with persistent expression of TGF-β1. It is possible that longer exposure to DMN prolonged expression of TGF-β1 in livers of medaka exposed to DMN for 4 weeks, promoting fibrosis and inhibiting tumor formation (proliferation of phenotypically altered hepatocytes) in these animals.

Pathological changes similar to those in rats given 3-day DMN intraperitoneal injections were apparent in the livers of medaka exposed to DMN for 2 and 4 weeks. These lesions included progressive hepatic necrosis, collapse of the hepatic architecture, inflammation, BPDEC (stem cell) hyperplasia, hepatic stellate cell hyperplasia, perisinusoidal collagen deposition, biliary duct hyperplasia and fibrosis, hepatocellular regeneration, and multinodular restructuring of the liver (Table 1, Figs. 3–11). Certain lesion patterns such as centrilobular necrosis and bridging (septal) fibrosis were absent in the medaka due to differences in the structure of the medaka liver versus rat (mammalian) liver. Medaka livers have the same cellular constituents and same basic structural/functional unit (portal tract, afferent blood flow and efferent bile flow, central/hepatic vein, and hepatic muralia) as rats. However, mammalian livers are composed of many lobules with multiple ''functional units,'' whereas the entire medaka liver is 1 lobule with 1 ''functional unit.''[15] In mammals, the enzyme responsible for the biotransformation of DMN (P450 2E1) is more concentrated in the centrilobular hepatocytes, increasing their susceptibility to DMN's hepatotoxic effects. DMN-induced centrilobular necrosis is an example of metabolic zonation in the mammalian liver.[20] Fish have a relatively homogeneous distribution of cytochrome P450s in their livers and, therefore, no metabolic zonation.[46] The diffuse distribution of biotransforming enzymes in medaka livers is presumably responsible for the random distribution of DMN-induced hepatocellular necrosis. Cirrhotic-like nodules similar to those that occur in DMN-exposed rats were present in some DMN-exposed medaka (Fig. 10), although, predictably, no consistent pattern of fibrosis was present given that the medaka liver is 1 functional unit (lobule).[13] Initial collagen deposition was similar between medaka and rats.[22] In medaka, collagen was deposited early as a fine, fibrillar matrix along the reticular framework of the denuded hepatic parenchyma. Matrix deposition was often accompanied by infiltration of spindle-shaped cells along residual reticular fibers. These same cells surrounded individual and/or clusters of degenerate hepatocytes (satellitosis) (Fig. 9). A similar pattern of spindle-cell proliferation has been reported in livers of Sprague-Dawley rats and Wistar rats exposed to DMN.[17,22] According to Jin et al.,[22] spindyloid (activated) HSCs migrated along the residual reticular framework of the necrotic liver. Early evidence of fibrosis was associated with diffuse distribution of the activated HSCs along the hepatic sinusoids in livers of DMN-exposed Wistar rats. Hepatic stellate cells are present in the medaka liver.[46] Laurén et al.[25] noted that the stellate processes of quiescent HSCs form the framework in which hepatocytes reside in the medaka liver. However, it is unclear on HE whether the ''spindle-shaped'' cells present in livers of DMN-exposed medaka represent activated HSCs, proliferating BPDECs, or a mixture of both (Fig. 9). In acutely necrotic livers of DMN-exposed medaka, hepatocellular loss was associated with maintenance of a ''honeycomb'' reticular framework, which may represent the stellate processes of HSCs that surrounded hepatocytes in these animals.

The biochemical alterations associated with DMN-induced hepatic injury and fibrosis in rats are well characterized and similar to what occurs in alcoholic cirrhosis in humans.[11,12,14] Transforming growth factor-β1 is the predominant profibrogenic stimulus.[7] Reactive oxygen intermediates (ROIs) released from macrophages and injured hepatocytes stimulate transdifferentiation of quiescent HSCs to contractile myofibroblasts. Injured endothelial cells convert latent TGF-β1 to the active, fibrogenic form through the activation of plasmin. TGF-β1 stimulates extracellular matrix (ECM; type-1 collagen) production by activating hepatic stellate cells. Smad-3, a cell-signaling protein of TGF-β1, is the mediator of TGF-β1's fibrogenic response, combining with other Smad proteins and translocating to the nucleus to affect gene transcription.[10,37] Activation of HSCs involves a phenotypic change and upregulation of α-SMA, which is an indication of its ECM-producing capabilities.[23] HSCs lay down collagen to facilitate healing of the hepatic parenchyma. The liver parenchyma regenerates and/or chronic injury leads to excessive matrix deposition and cirrhosis.[2,11] TGF-β1 also has an antiproliferative effect.[10] Hepatic progenitor cells are more sensitive to TGF-β1 expression than are oval cells (stem cells) in rats. Presumably, the injured hepatic parenchyma is replaced via oval cell lineage and not hepatic progenitor cells given their suppression by TGF-β1.[29,32] TGF-β1 and Smad-3 are also potent inhibitors of cell progression at the G1 phase.[29,30] Altered regulation of TGF-β1 is thought to be important in some cases of HCC.[2] In the present study, histochemical and immunohistochemical stains were used to determine whether biochemical alterations were present in the livers of DMN-exposed medaka that were similar to those processes known to occur in rats exposed to DMN and human alcoholic cirrhosis. Although positive staining is not definitive evidence of genetic expression, it does suggest upregulation of cellular markers that can be

indicative of a DMN-induced response in fish tissue. Medaka tissues were stained for TGF-β1, Smad-3, cytokeratin (AE1/AE3), Sirius red, reticulin, MSA, and GFAP (Tables 4, 5). Initial attempts at staining medaka tissue with α-SMA and factor VIII were unsuccessful and were not included in the final staining regimen.

Livers of DMN-exposed medaka stained positively with the TGF-β1 antibody. Positive staining was evident in the cytoplasm of BPDECs, intermediate cells, immature hepatocytes, and mature hepatocytes. This is in comparison to control fish, in which only scattered BPDECs stained positively for TGF-β1. The staining of hepatocytes for TGF-β1 associated with DMN-induced injury in medaka livers is similar to that which occurs in rats and humans and suggests a role for this cytokine in hepatic repair mechanisms in fish.[5,42] In control rats, only Kupffer cells and sinusoidal endothelial cells stain positively in the normal liver. It is unclear why BPDECs stain positively for TGF-β1 in the livers of control medaka. It has been reported that cholangiocytes are a source of the profibrogenic cytokine TGF-β2, an isoform of TGF-β1.[36,37] The TGF-β1 antibody used on medaka livers, although labeled as TGF-β1 specific, has cross-reactivity with TGF-β2. It is possible that the TGF-β1 antibody was linking with TGF-β2 on the cell surfaces of BPDECs in the control fish. However, staining of BPDECs for TGF-β1 in DMN-exposed medaka was increased in comparison to control fish. In rats, bile duct ligation induces proliferation of biliary epithelial cells that stain strongly positive for TGF-β1; these cells promote fibrogenesis via transdifferentiation of peribiliary fibroblasts and HSCs.[44] It is possible that the positive staining of BPDECs with TGF-β1 indicates TGF-β1 expression by these cells, not cross-reactivity with TGF-β2, and potentially a fibrogenic role for BPDECs in DMN-exposed medaka. In addition, many BPDECs and intermediate cells stained positively for TGF-β1 within neoplastic foci of DMN-exposed medaka (Figs. 25, 26). In the Solt-Farber and choline-deficiency carcinogenic protocols, designed to study the development and relationship of foci and nodules as precursor lesions to HCCs, bipolar ductal progenitor cells and small periductal cells appear to be the HCC cells of origin.[40] Positive staining of BPDECs and intermediate cells in hepatic neoplastic nodules of some DMN-exposed medaka can indicate a stem cell origin for hepatic neoplasms in these animals. This is in contrast to HCCs arising from phenotypically altered and dysplastic hepatocytes.[45] Positive staining with Smad-3 was less definitive in DMN-exposed medaka; however, general patterns of increased hepatocellular cytoplasmic and nuclear staining corresponded with regions of increased hepatocellular and/or biliary staining with TGF-β1. This is consistent with findings reported for TGF-β1 and Smad-3 expression in hepatocytes of human patients with chronic liver disease.[5] Nuclear staining, indicating translocation of Smad-3 to the hepatocyte nucleus, was rare but was present in some liver sections of DMN-exposed medaka. Some fish demonstrated decreased Smad-3 staining of neoplastic cells in association with increased staining of TGF-β1, which suggests disruption of the TGF-β1 pathway and loss of responsiveness to TGF-β1's antiproliferative effects. It is thought that altered regulation TGF-β1 (decreased inhibition to growth inhibitory signals) and not decreased expression is responsible for formation of some HCCs in humans.[2,38] In 1 fish, however, TGF-β1 and Smad-3 staining was decreased in neoplastic hepatocytes (HCCs), suggesting decreased expression of TGF-β1 in the neoplasm of this fish. Proliferating BPDECs and intermediate cells stained intensely with cytokeratin antibody (Figs. 27, 30). In some liver sections, proliferation and staining of these cells were quite extensive. Cytokeratin-positive BPDECs and intermediate cells densely infiltrated the hepatic parenchyma along hepatic plates and denuded reticular framework, supporting their role in regeneration of the hepatic parenchyma.[34] Often a fine, fibrillar network of collagen, evident with the Sirius red stain, accompanied the parenchymal infiltration of BPDECs and intermediate cells (Fig. 29); it is possible that TGF-β1 expression by these cells induced a fibrogenic response in local transdifferentiated HSCs and/or peribiliary fibroblasts. Thicker bands of collagen were also evident with the Sirius red stain (Fig. 28), occasionally accompanied by spindle cell proliferation (presumed biliary origin). Increased staining of type III collagen (reticular) fibers by the reticulin silver stain often correlated with Sirius red staining, supporting increased collagenous matrix deposition and restructuring of hepatic architecture in response to DMN-induced hepatic injury (Fig. 31). Perisinusoidal staining with MSA in DMN-treated medaka was marginally successful (Fig. 32). This was consistent with the finding reported by Bunton[4] for medaka exposed to DEN and methylmazoxymethanol acetate (MAM-Ac). Periductal staining of fibroblasts with MSA was more often apparent than positive perisinusoidal staining, indicative of activated HSCs, although positive staining of activated HSCs with MSA only occurred in DMN-treated fish and not in controls. Jin et al.[22] noted that positive staining of activated HSCs with α-SMA in DMN-exposed Wistar rats was time dependent. Activated HSCs migrating into the necrotic hepatic parenchyma stained for α-SMA at day 5 post DMN injection; however, activated HSCs were negative at 14 days post injection when the necrotic parenchyma was replaced by regenerating hepatocytes and fibrosis. It is possible that MSA expression by activated HSCs in DMN-exposed medaka is also time dependent and that positive staining of HSCs with MSA would have been more significant at an early time point. In mammals, quiescent HSCs stain positively for GFAP. Medaka HSCs did not stain with GFAP in either control or DMN-injured livers; however, GFAP successfully stained neural tissue in treated and control medaka. Negative staining of HSCs with GFAP can indicate structural and/or functional differences between medaka (or fish) HSCs and mammalian HSCs. Quiescent HSCs in cod have been reported to stain positively for cytokeratin.[41] Intense pericellular staining occurred with the cytokeratin antibody in DMN-exposed medaka (Fig. 30); however, it is unlikely that this represents positive staining of transdifferentiated HSCs (myofibroblasts phenotype) for cytokeratin, since quiescent (epithelial phenotype) HSCs did not stain for cytokeratin in control medaka.

## Summary

Our goal in this study was to determine (descriptively and mechanistically) whether DMN-induced hepatic injury and carcinogenesis in medaka were comparable to DMN-induced hepatic cirrhosis and carcinogenesis in rodents. We found that despite differences in the hepatic architecture of medaka and rats, DMN-induced changes were similar in both species, particularly when evaluated at the cellular level. Although transcriptional evidence (such as obtained by reverse transcription–polymerase chain reaction) is necessary for more definitive conclusions concerning comparable biochemical alterations for DMN-exposed medaka and rats, the histochemical and immunohistochemical data suggest a similar mechanism for repair of DMN-induced hepatic injury and possibly hepatic neoplasia in both species. Morphological comparisons accompanied by mechanistic data will improve interspecies comparisons across divergent phylogenies. However, despite common morphologic changes and biochemical alterations, fish may not always be appropriate as alternative animal models for human disease, particularly when a model depends on pattern-specific pathology that is in part determined by species–specific hepatic architecture.

### Acknowledgements

We thank Drs. David Malarkey, David Hinton, and Arnaud Van Wettere for their valuable contributions and comments on the manuscript. Dr. Hinton has been a valuable "medaka team member." As always, we thank Sandra Horton, Monica Matmeuller, and the entire staff of the Histopathology Laboratory at the NCSU College of Veterinary Medicine for their wonderful expertise in fish histology, immunohistochemistry, and cheerful attitude. Dr. Law is a member of the NCSU Center for Comparative Medicine and Translational Research. This manuscript is submitted in partial fulfillment of the degree of Doctor of Philosophy granted to Dr. Kristen R. Hobbie. This manuscript has been reviewed by the Environmental Protection Agency and approved for publication. Mention of trade names or commercial products does not constitute endorsements or recommendations for use.

### Declaration of Conflicting Interests

The authors declared no potential conflicts of interest with respect to the research, authorship, and/or publication of this article.

### Funding

The authors disclosed receipt of the following financial support for the research, authorship, and/or publication of this article: funding from the State of North Carolina institutional research funds, the NCSU CVM graduate program in Comparative Biomedical Sciences, and the inter-institutional funding agreement between NC State University and the US EPA, Research Triangle Park, North Carolina.

### References

1. Bailey GS, Williams DE, Hendricks JD. Fish models for environmental carcinogenesis: the rainbow trout. *Environ Health Perspect.* 1996;104(suppl 1):5-21.
2. Bissell DM, Roulot D, George J. Transforming growth factor β and the liver. *Hepatology*. 2001;34:859-867.
3. Boorman GA, Botts S, Bunton TE, et al. Diagnostic criteria for degenerative, inflammatory, proliferative nonneoplastic and neoplastic liver lesions in medaka (*Oryzias latipes*): consensus of a National Toxicology Program pathology working group. *Toxicol Pathol*. 1997;25:202-210.
4. Bunton TE. Expression of actin and desmin in experimentally induced hepatic lesions and neoplasms from medaka (Oryzias latipes). *Carcinogenesis*. 1995;16:1059-1063.
5. Calabrese F, Valente M, Giacometti C, et al. Parenchymal transforming growth factor beta-1: its type II receptor and Smad signaling pathway correlate with inflammation and fibrosis in chronic liver disease of viral etiology. *J Gastroenterol Hepatol*. 2003;18:1302-1308.
6. Cutroneo KR, White SL, Chiu J-F, Ehrlich HP. Tissue fibrosis and carcinogenesis: divergent or successive pathways dictate multiple molecular therapeutic targets for oligo decoy therapies. *J Cell Biochem.* 2006;97:1161-1174.
7. De Gouville A-C, Boullay V, Krysa G, et al. Inhibition of TGF-β signaling by an ALK 5 inhibitor protects rats from dimethylnitrosamine-induced liver fibrosis. *Br J Pharmacol.* 2005; 145:166-177.
8. Dick A, Mayr T, Hermann B, Meier A, Hammerschmidt M. Cloning and characterization of zebrafish *smad2*, *smad3* and *smad4*. *Gene*. 2000;246:69-80.
9. Elliot EL, Blobe GC. Role of transforming growth factor beta in human cancer. *J Clin Oncol.* 2005;23:2078-2093.
10. Flanders KC. Smad3 as a mediator of the fibrotic response. *Int J Exp Path*. 2004;85:47-64.
11. Friedman SL: Molecular regulation of hepatic fibrosis, an integrated cellular response to injury. *J Biol Chem.* 2000;275:2247-2250.
12. George J. Mineral metabolism in dimethylnitrosamine-induced hepatic fibrosis. *Clin Biochem.* 2006;39:984-991.
13. George J, Tsutsumi M, Takase S. Expression of hyaluronic acid in *N*-nitrosodimethylamine induced hepatic fibrosis in rats. *Int J Biochem Cell Biol.* 2004;36:307-319.
14. Grieco MP, Hendricks JD, Scanian RA, Sinnhuber RO, Pierce DA. Carcinogenicity and acute toxicity of dimethylnitrosamine in rainbow trout (*Salmo gairdneri*). *J Natl Cancer Inst.* 1978;60:1127-1131.
15. Hardman RC, Volz DC, Kullman SW, Hinton DE. An in vivo look at vertebrate liver architecture: three-dimensional reconstructions from medaka (Oryzias latipes). *Anat Rec.* 2007;290:770-782.
16. Harms CA, Kennedy-Stoskopf S, Horne WA, Fuller FJ, Tompkins WAF. Cloning and sequencing hybrid striped bass (Morone saxatilis x M. chrysops) transforming growth factor-β (TGF-β), and development of a reverse transcription quantitative competitive polymerase chain reaction (RT-qcPCR) assay to measure TGF-β mRNA of teleost fish. *Fish Shellfish Immunol.* 2000;10:61-85.
17. Hata J, Ikeda E, Uno H, Asano S. Expression of hepatocyte growth factor mRNA in rat liver cirrhosis induced by N-nitrosodi methylamine as evidenced by in situ RT-PCR. *J Histochem Cytochem.* 2002;50:1461-1468.
18. Hawkins WE, Walker WW, Fournie JW, Manning CS, Krol RM. Use of the Japanese medaka (*Oryzias latipes*) and Guppy (*Poecilia reticulata*) in carcinogenesis testing under National Toxicology Program protocols. *Toxicol Pathol.* 2003;31(suppl 1):88-91.

19. He J-Y, Ge W-H, Chen Y. Iron deposition and fat accumulation in dimethylnitrosamine-induced liver fibrosis in rat. *World J Gastroenterol*. 2007;13:2061-2065.
20. Hinton DE, Segner H, Braunbeck T. Toxic responses of the liver. In: Schlenk D, Benson WH, eds. *Target Organ Toxicity in Marine and Freshwater Teleosts*. 1st ed. New York, NY: Taylor & Francis; 2001:224-261.
21. Hobbie KR, Deangelo AB, King LC, Winn RN, Law JM. Toward a molecular equivalent dose: use of the medaka model in comparative risk assessment. *Comp Biochem Physiol C Toxicol Pharmacol*. 2009;149:141-151.
22. Jin Y-L, Enzan H, Kuroda N, et al. Tissue remodeling following submassive hemorrhagic necrosis in rat livers induced by an intraperitoneal injection of dimethylnitrosamine. *Virchows Arch*. 2003;442:39-47.
23. Kang JS, Morimura K, Salim EI, Wanibuchi H, Yamaguchi S, Fukushima S. Persistence of liver cirrhosis in association with proliferation of nonparenchymal cells and altered location of α-smooth muscle actin-positive cells. *Toxicol Pathol.* 2005;33:329-335.
24. Khudoley, VV. Use of aquarium fish, *Danio rerio* and *Poecilia reticulata*, as test species for evaluation of nitrosamine carcinogenicity. *J Natl Cancer Inst*. 1984;65:65-70.
25. Laurén DJ, The SJ, Hinton DE. Cytotoxicity phase of diethylnitrosamine-induced hepatic neoplasia in medaka. *Cancer Res*. 1990;50:5504-5514.
26. Law JM. Mechanistic considerations in small fish carcinogenicity testing. *ILAR J*. 2001;42:274-284.
27. Law JM. Issues related to the use of fish models in toxicologic pathology: session introduction. *Toxicol Pathol.* 2003; 31(suppl):49-52.
28. Lim Y-S, Kim K-A, Jung J-O, et al. Modulation of cytokeratin expression during in vitro cultivation of human hepatic stellate cells: evidence of transdifferentiation from epithelial to mesenchymal phenotype. *Histochem Cell Biol*. 2002;118:127-136.
29. Lowes KN, Croager EJ, Olynyk JK, Abraham LJ, Yeoh GCT. Oval cell-mediated liver regeneration: role of cytokines and growth factors. *J Gasteroenterol Hepatol*. 2003;18:4-12.
30. Matsuura I, Denissova NG, Wang G, He D, Long J, Liu F. Cyclin-dependent kinases regulate the antiproliferative function of Smads. *Nature*. 2004;430:226-231.
31. Mizgireuv IV, Majorova IG, Gorodinskaya VM, Khudoley VV, Revskoy SY. Carcinogenic effect of N-nitrosodimethylamine on diploid and triploid zebrafish (Danio rerio). *Toxicol Pathol.* 2004;32:514-518.
32. Nguyen LN, Furuya MH, Wolfraim LA, et al. Transforming growth factor-beta differentially regulates oval cell and hepatocyte proliferation. *Hepatology*. 2007;45:31-41.
33. Okihiro MS, Hinton DE. Progression of hepatic neoplasia in medaka (Oryzias latipes) exposed to diethylnitrosamine. *Carcinogenesis*. 1999;20:933-940.
34. Okihiro MS, Hinton DE. Partial hepatectomy and bile duct ligation in rainbow trout (Oncorhynchus mykiss): histologic, immunohistochemical and enzyme histochemical characterization of hepatic regeneration and biliary hyperplasia. *Toxicol Pathol.* 2000;28:342-356.
35. Peto R, Gray R, Brantom P, Grasso P. Effects on 4080 rats of chronic ingestion of N-nitrosodiethylamine or N-nitrosodimethylamine: a detailed dose-response study. *Cancer Res*. 1991; 51:6415-6451.
36. Popov Y, Patsenker E, Fickert P, Trauner M, Schuppan D. Mdr2 (Abcb4)-/- mice spontaneously develop severe biliary fibrosis via massive dysregulation of pro- and antifibrogenic genes. *J Hepatol*. 2005;43:1045-1054.
37. Roberts AB, Tian F, DaCosta Byfield S, et al. Smad3 is key to TGF-β-mediated epithelial-to-mesenchymal transition, fibrosis, tumor suppression and metastasis. *Cytokine Growth Factor Rev*. 2006;17:19-27.
38. Rossmanith W, Schulte-Hermann R. Biology of transforming growth factor β in hepatocarcinogenesis. *Microsc Res Tech*. 2001;52:430-436.
39. Sato Y, Harada K, Ozaki S, et al. Cholangiocytes with mesenchymal features contribute to progressive hepatic fibrosis of the polycystic kidney rat. *Am J Pathol*. 2007;171: 1859-1871.
40. Sell S. Cellular origin of hepatocellular carcinomas. *Cell Dev Biol*. 2002;13:419-424.
41. Senda T, Nomura R. The expression of cytokeratin in hepatic stellate cells of the cod. *Arch Histol Cytol*. 2003;66:437-444.
42. Song S-L, Gong Z-J, Zhang Q-R, Huang T-X. Effects of Chinese traditional compound, JinSanE, on expression of TGF-β1 and TGF-β1 type II receptor mRNA, Smad3 and Smad7 on experimental hepatic fibrosis in vivo. *World J Gasterenterol*. 2005;11:2269-2276.
43. Souliotis VL, Chhabra S, Anderson LM, Kyrtopoulos SA. Dosimetry of O6-methylguanine in rat DNA after low-dose, chronic exposure to N-nitrosodimethylamine (NDMA): implications for the mechanism of NDMA hepatocarcinogenesis. *Carcinogenesis*. 1995;16:2381-2387.
44. Tao L-H, Enzan H, Hayashi Y, et al. Appearance of denuded hepatic stellate cells and their subsequent myofibroblasts-like transformation during the early stage of biliary fibrosis in the rat. *Med Electron Microsc*. 2000;33:217-230.
45. Thorgeirsson SS, Grisham JW. Molecular pathogenesis of human hepatocellular carcinoma. *Nat Genet*. 2002;31: 339-346.
46. Wolf JC, Wolfe MJ. A brief overview of nonneoplastic hepatic toxicity in fish. *Toxicol Pathol.* 2005;33:75-85.